

Multiple-Input Multiple-Output Enabled Large Bandwidth Density On-Chip Optical Interconnect

Po-Kuan Shen, Amir Hosseini, Xiaochuan Xu, Yongqiang Hei, Zeyu Pan, *Student Member, IEEE*,
and Ray T. Chen, *Fellow, OSA*

Abstract—We propose to apply the multiple-input multiple-output (MIMO) from wireless communication to high density on-chip optical interconnect. MIMO makes it possible to reduce the waveguide pitch to subwavelength range and uses the crosstalk to improve system performance. The proposed $N \times N$ on-chip MIMO system consists of transmitter, high-density waveguides, homodyne coherent receivers, and electrical signal processing components. As an example, a 10×10 MIMO system with waveguide spacing of 250 nm is simulated. The possibility of data transmission at 10 Gb/s/channel from high-density waveguide array is numerically investigated. The minimum input optical power for the BER of 10^{-12} can reach -18.1 dBm. The BER is better than 10^{-12} when there is a phase shift of 73.5° . Compared to the conventional parallel waveguides with $2\text{-}\mu\text{m}$ pitch, the bandwidth density can be enhanced from 5 to 13.33 Gbit/ $\mu\text{m/s}$ at 10 Gb/s by using the MIMO techniques.

Index Terms—Optical interconnections, optical waveguides, silicon photonics.

I. INTRODUCTION

OPTICAL interconnects are expected to be widely used in next generation on-chip interconnects because of the superior advantages in propagation delay, energy consumption, and bandwidth density compared to electrical solutions [1], [2]. Driven by the continuous increase of the integration density and complexity, there is growing interest in further improving the bandwidth density without consuming more chip area. [3] Inspired by the mode-division multiplexing (MDM) in few-mode fibers, a few attempts have been made to incorporate the MDM into on-chip optical interconnects. [3], [4] While MDM adds spatial-mode-parallelism degree of freedom, it also places a few constrains. For example, to suppress the mode conversion induced crosstalk, the number of modes and the length of the waveguide are limited, and waveguide bending must be avoided. Considering on-chip optical interconnects are usually

Manuscript received July 16, 2015; revised November 23, 2015 and January 15, 2016; accepted February 2, 2016. Date of publication February 10, 2016; date of current version June 1, 2016. This work was supported in part by Ministry of Science and Technology, Taiwan, under Graduate Student Study Abroad Program under Grant 103-2917-1-008-042.

P.-K. Shen is with the Department of Optics and Photonics, National Central University, Jhongli 32001, Taiwan, and also with the Department of Electrical and Computer Engineering, University of Texas, Austin, TX 78758 USA (e-mail: pokuanshen@gmail.com).

A. Hosseini and X. Xu are with the Omega Optics, Inc., Austin, TX 78757 USA (e-mail: amir.hosseini@omegaoptics.com; xiaochuan.xu@omegaoptics.com).

Y. Hei, Z. Pan, and R. T. Chen are with the Department of Electrical and Computer Engineering, University of Texas, Austin, TX 78758 USA (e-mail: yqhei@utexas.edu; panzeyu@utexas.edu; raychen@uts.cc.utexas.edu).

Color versions of one or more of the figures in this paper are available online at <http://ieeexplore.ieee.org>.

Digital Object Identifier 10.1109/JLT.2016.2527721

considered as an alternative to electrical bus, the limit of the transmission distance is particularly catastrophic. Improving bandwidth in a single channel is also a possible solution to increase the bandwidth density in on-chip optical interconnects. However, signal multiplexing must be adopted to fully utilize such a large bandwidth of a single channel, which inevitably increases system complexity and cost. High density parallel channel waveguides is another possible solution. However, the bandwidth density of optical waveguides is ultimately determined by the waveguide geometry and index contrast between the waveguide core and cladding [5]. CMOS-compatible single mode silicon waveguides have submicrometer dimensions due to the high index contrast between silicon and its cladding material [6]–[8]. As the shrinkage of the width of the waveguide is not physically possible, reducing the channel spacing is an intuitive alternative. To avoid crosstalk, conventional silicon waveguides must be placed several microns apart from each other, which is a great waste of precious chip area. According to Ref [9], reducing the space between parallel waveguides from 3 to 1 μm can potentially save $\sim 57\%$ of chip area wasted for routing. However, further decrease the waveguide spacing is very challenging.

In this letter, we proposed and investigated the possibility of using multiple-input multiple-output (MIMO) to further reduce the waveguide spacing and improve the bandwidth density of on-chip optical interconnects. MIMO has been extensively used in wireless communications for a long time. MIMO in optics also has been studied for decades. The MIMO transmissions employ different modes of multi-mode fiber (MMF) to establish different data channels. Hence higher transmission capacity can be achieved and the mode dispersion can be avoided. For example, a gross transmission throughput of 255 Tb/s over a 1 km fiber link is implemented by using few-mode multicore fiber and MIMO technique [10]. However, the research activities only focus on its applications in optical fiber communications, especially MMF based local area networks [11]–[14]. According to the authors' best knowledge, this is the first time MIMO has been studied for on-chip interconnects. MIMO shows that it is possible to make use of the crosstalk to improve the system performance instead of avoiding it [15], [16]. Using the MIMO technique, several data streams can be transmitted simultaneously over the same multiple parallel paths. Each receiver catches the combination of transmitted data, and then the electrical signal processing techniques is used to decode the transmitted signal.

If each guiding mode in the high density waveguide region is considered as a signal path, the high density waveguide array behaves similar to a wireless channel with tense multipath scattering. Using MIMO techniques, the waveguide array no longer

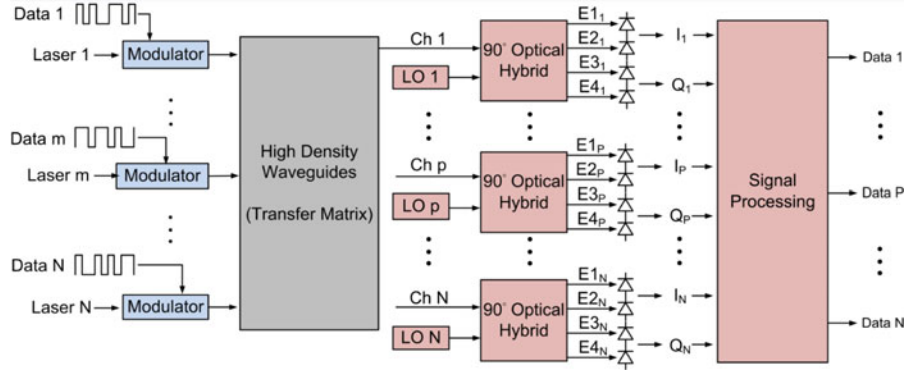


Fig. 1. The block diagram of proposed $N \times N$ on-chip MIMO system operating over the high density silicon waveguide array.

need to be kept physically decoupled. The waveguide pitch can be significantly reduced to subwavelength range and therefore the bandwidth density can be improved further. Moreover, the proposed on-chip MIMO system uses the conventional waveguides and avoids the complex and sensitive couplers. There are no fundamental limits on the length, bends, and number of channels in the on-chip MIMO. An $N \times N$ on-chip MIMO system is analyzed in this letter, and as an example we simulated 10 heavily coupled waveguides with 250 nm spacing to perform the data transmission of 10 Gb/s/channel.

The paper is organized as: the design of on-chip MIMO system, including high density waveguides, homodyne coherent receiver, and electrical signal processing, are discussed first in Section 2. In Section 3, as an example, we simulate and discuss the performance of 10×10 on-chip MIMO system. The 10 Gb/s/channel data transmissions from high density waveguide array are numerically investigated, including waveform recovery and eye diagram. To evaluate the performance of whole system, we also discuss the input optical power requirement and phase shift between input laser and local oscillator in the Section 3. Finally, we will conclude the paper in Section 4.

II. DESIGN OF ON-CHIP MIMO SYSTEM

Fig. 1 shows the block diagram of the proposed $N \times N$ on-chip MIMO system, which consists of transmitters, N high density waveguides, homodyne coherent receivers, and electrical signal processing components. In the transmitters, each input laser, which has the same wavelength, phase, and optical power, is launched into the individual optical amplitude modulator and then fed into the high density silicon waveguide array. In the N high density waveguides, there is significant coupling among the adjacent waveguides due to the subwavelength waveguide pitch. It causes that number of signal streams is transmitted simultaneously over the same multipath channels, so that the signal streams randomly combined in each receiver. The relation between input ports and output ports can be described as

$$\begin{bmatrix} O_1 \\ \vdots \\ O_p \\ \vdots \\ O_N \end{bmatrix} = \begin{bmatrix} T_{11} & \dots & T_{1m} & \dots & T_{1N} \\ \vdots & & \vdots & & \vdots \\ T_{p1} & \dots & T_{pm} & \dots & T_{pN} \\ \vdots & & \vdots & & \vdots \\ T_{N1} & \dots & T_{Nm} & \dots & T_{NN} \end{bmatrix} \begin{bmatrix} I_1 \\ \vdots \\ I_m \\ \vdots \\ I_N \end{bmatrix}. \quad (1)$$

Here, $[T_{pm}]$ is the transfer matrix of high density waveguides, $[I_m]$ is the electrical field at m -th input port, and $[O_p]$ is the electrical field at p th output port. Due to the nature of the coupling between waveguides, the elements of the transfer matrix are independent. All matrix elements are complex numbers as they take into account both amplitude and phase of electric field at each input and output port of the high density silicon waveguide array. In the experiment, the elements of the transfer matrix can be obtained by the standard calibration procedure established in MMF based MIMO systems. This calibration process will be done at initial stage, and most disturbances, such as the fabrication errors of waveguide and quadrature optical hybrid, can be relieved by the calibration.

Then the homodyne coherent receiver is used to detect the full electric field of transmitted signals, which contains both amplitude and phase information. In the homodyne coherent receiver, the local oscillator which has the same frequency, phase, and amplitude as input laser are the key to lock the phase of the incoming optical signals and serve as an absolute phase reference [17]. The superposed electrical field (O_p) from each input channels and local oscillator (E_{Lp}) are directed into the quadrature optical hybrid which gives four outputs:

$$E_{1p} = \frac{1}{2} (O_p + E_{Lp}) = \frac{1}{2} \left(\sum_{m=1}^N T_{pm} I_m + E_{Lp} \right) \quad (2)$$

$$E_{2p} = \frac{1}{2} (O_p - E_{Lp}) = \frac{1}{2} \left(\sum_{m=1}^N T_{pm} I_m - E_{Lp} \right) \quad (3)$$

$$E_{3p} = \frac{1}{2} (O_p + jE_{Lp}) = \frac{1}{2} \left(\sum_{m=1}^N T_{pm} I_m + jE_{Lp} \right) \quad (4)$$

$$E_{4p} = \frac{1}{2} (O_p - jE_{Lp}) = \frac{1}{2} \left(\sum_{m=1}^N T_{pm} I_m - jE_{Lp} \right). \quad (5)$$

By applying (2), (3), (4), and (5) to four PIN photodetectors (PDs), it provides the I_p and Q_p components which is given by

$$\begin{aligned} I_p &= I_{E_{1p}} - I_{E_{2p}} \\ &= R \sum_{m=1}^N \sqrt{P_{pm} P_{Lp}} \cos(\theta_{pm} - \theta_{Lp}) \end{aligned} \quad (6)$$

$$\begin{aligned} Q_p &= I_{E_{3p}} - I_{E_{4p}} \\ &= R \sum_{m=1}^N \sqrt{P_{pm} P_{Lp}} \sin(\theta_{pm} - \theta_{Lp}). \end{aligned} \quad (7)$$

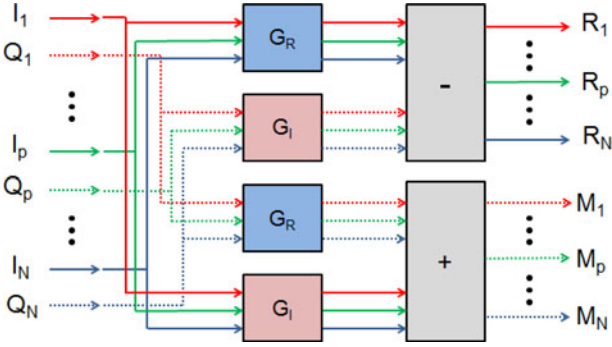


Fig. 2. The schematic of the signal processing for the $N \times N$ on-chip MIMO.

Here, R is the responsivity of PD, P_{pm} is the optical power from m th input port to p th output port, P_{Lp} is the optical power of local oscillator at p th receiver, θ_{pm} is the phase of received signal from m th input port to p th output port, and the θ_{Lp} is phase of local oscillator at p th receiver. I_p and Q_p represent the PD current from optical signals in phase and $\pi/2$ out of phase with local oscillator, respectively. Since the amplitude and phase information of the transmitted signal could be detected, these are applied to recover the transmitted signal in signal processing.

Fig. 2 shows the schematic of the signal processing, which consists of two steps: 1) calculating the real parts (G_R) and imaginary parts (G_I) of inverse transfer matrix; 2) using the inverse transfer matrix to calculate the recovered data. The calculated formulas are shown below:

$$R_p = I_p \times G_R - Q_p \times G_I \quad (8)$$

$$M_p = Q_p \times G_R + I_p \times G_I. \quad (9)$$

Both I_p and Q_p from the homodyne coherent receivers are branched into the real parts and imaginary parts of inverse transmission matrix, respectively. The adder and subtractor are used to calculate the real parts (R_p) and imaginary parts (M_p) of recovered data. It enables the signal to transmit from multiple input ports and receive by multiple output ports. Although many signal recover methods have been developed in wireless MIMO systems, such as minimum mean square error and maximum ratio combining, we found the channel inversion method discussed above is very effective in the heavily coupled parallel waveguide system. The introduce of coherent detection techniques also greatly improves the system performance. [13]

III. 10×10 MIMO SYSTEM

Based on the above discussion, we simulated the performance of a 10×10 on-chip MIMO system comprised of ten silicon strip waveguides, coherent detection, and signal processing. The MODE Solution Package from Lumerical software Inc. is used to simulate the ten high density waveguides and calculate the transfer matrix of high density parallel silicon waveguides. Fig. 3(a) schematically shows the cross-section of the ten high density parallel silicon waveguides on SOI substrate. The cross section ($W \times H$) of each Si waveguide is 500×220 nm with a refractive index of 3.4764. The spacing (S) is 250 nm. The waveguide length is 1 mm. The thickness of buried oxide (BOX)

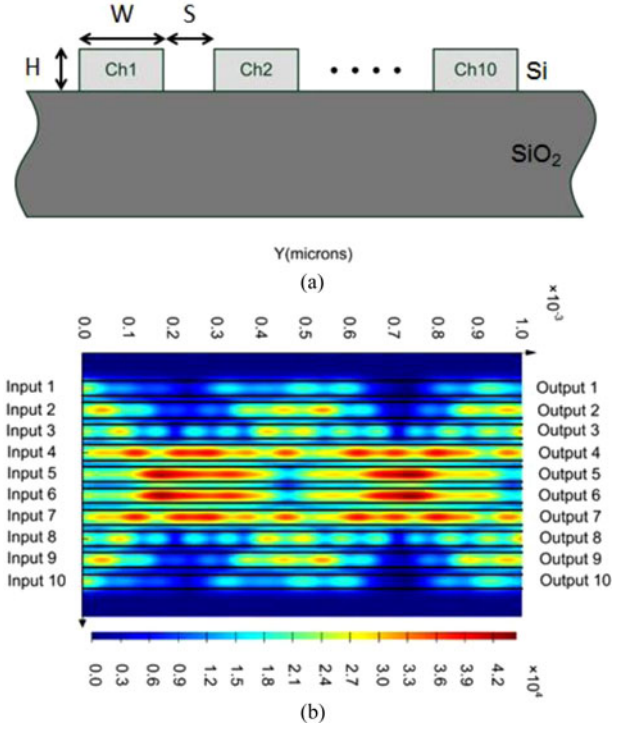


Fig. 3. (a) The schematic cross-section of ten high density parallel silicon waveguides with 250 nm spacing (b) The electric field magnitude distribution in the ten high density parallel silicon waveguides.

layer is $2 \mu\text{m}$ and its refractive index is 1.444 [18]. Fig. 3(b) shows the simulated electric field magnitude distribution of the ten high density waveguides at 1550 nm. The mode coupling between adjacent waveguides is strong due to the extremely small waveguide spacing. In order to define the inverse transfer matrix for the electrical signal process, we calculate the transfer matrix of the coupled-ten waveguides. It is obtained by sequentially exciting each waveguide with the fundamental TE mode and records the amplitude and phase of the electric field at each output port. From the simulation result, the transfer matrix is not unitary. It comprises of all the coupled modes and also considers entire waveguide loss (including mode-dependent loss [19]). Although there is a slight waveguide loss, the inverse transfer matrix and electrical signal processing can be used to compensate these excess waveguide losses.

A. Data Recovery of 10×10 On-Chip MIMO System

To verify the 10×10 on-chip MIMO system, we used the INTERCONNECT package from Lumerical software Inc. to simulate the whole system, including waveform recovery, eye diagram, input optical power requirement, and phase shift between input laser and local oscillator. In the simulation model, the high density waveguides are replaced by the 10×10 transfer matrix. In the transmitter part, each input channel has an independent electrical signal source and a randomly electrical noise source. The ten lasers with wavelength of 1550 nm, relative intensity noise of -145 dB/Hz, and optical power of 0 dBm are fed into optical amplitude modulators which are modulated by 10 Gb/s non-return-to-zero high-speed electrical

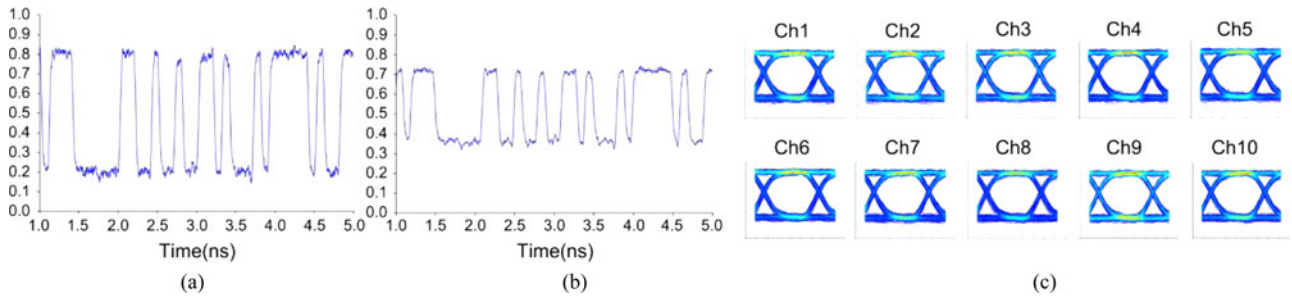


Fig. 4. (a) The input electrical signal waveform in the channel 5. The electrical noise source and random jitter of 1.5 ps is used to define the quality factor of input electrical signals. (b) The recovered signal waveform in the channel 5. (c) The recovered eye diagram for 10×10 on-chip MIMO system.

signals with a pseudo-random bit sequence of $2^{31}-1$ and quality factor of 16. All of these values refer to the Agilent N4872A ParBERT modules and the commercial distributed feedback lasers [20], [21]. In the receiver part, the local oscillators possess the same characteristic as input laser. The PDs with responsivity of 0.8 W/A, dark current of 10 nA, and thermal noise of 10^{-22} are utilized to detect the transmitted optical signals. The 3-dB frequency bandwidth of PDs is 22 GHz (Discovery Semiconductors DSC30S). Fig. 4 shows the comparison of eye diagram and waveform between input electrical signals and output recovered signals. Fig. 4(a) is the waveform of the input electrical signal in channel 5. The amplitude of input electrical signal is 0.6 a.u.. The noise caused by the internal electrical noise source and random jitter of 1.5 ps is used to define the quality factor of input electrical signals. Fig. 4(b) shows the recovered signal waveform. The simulation proves that it is possible to recover signals from ten heavily coupled waveguides with 250 nm spacing. Compared to the input signals, the amplitude of recovered waveform approximately reduce to 0.35 a.u., it's due to the PDs responsivity of 0.8 A/W and the electrical signal processing. Fig. 4(c) shows the recovered eye diagram at 10 Gb/s/channel. The peak-to-peak jitter is 10.69 ps. The clear eye diagrams demonstrate that the proposed on-chip MIMO system possess the facility in data transmission at 10 Gb/s/channel. For the conventional 10 mm parallel waveguides without MIMO, the cross-section dimensions require offering $2 \mu\text{m}$ pitches to avoid crosstalk [22], and the bandwidth density is 5 Gbit/ $\mu\text{m}/\text{s}$ at 10 Gb/s data rate. Using the MIMO techniques, the bandwidth density can be enhanced from 5 to 13.33 Gbit/ $\mu\text{m}/\text{s}$ at 10 Gb/s data rate. The footprint of waveguides can be reduced from 0.23 to 0.0725 mm^2 ($\sim 68\%$), while the 90° hybrid and additional PD in coherent detection will consume 0.0078 and 0.00014 mm^2 per channel, respectively [23], [24]. Although coherent detection is more complicated than intensity detection, the proposed on-chip MIMO systems still have smaller total footprint in the on-chip global interconnects because of the use of high density parallel waveguides. Note that the bandwidth density and waveguide footprint in the proposed MIMO on-chip optical interconnects could be further improved if the waveguide space keep reducing. Although the smaller waveguide space will induce stronger mode coupling, and lead to that the transfer matrix becomes less diagonally dominant, the signals can still be recovered through the proposed on-chip MIMO. [12]

B. Performance Evaluation of 10×10 On-Chip MIMO System

Most solutions to improve integration density and bandwidth density rely on waveguide design, such as waveguide shape, waveguide length, or the relationship between adjacent waveguides. The proposed on-chip MIMO does not strongly depend upon these parameters because it uses the inverse transfer matrix based electrical signal processing. All waveguide characteristics, such as mode coupling, have been considered in the transfer matrix. Therefore, instead of studying the impact of waveguide parameters, we investigate the impact of system parameters, including input power, waveguide numbers, and phase errors. In this section, we simulate the bit error rate (BER) as a function of the input optical power for the 3×3 , 5×5 , and 10×10 on-chip MIMO system. In the simulation model, the laser lightwave feeds into the individual variable optical attenuator and passes through the high density waveguide array. Then the optical attenuators are adjusted and then the input optical power requirement can be characterized. Fig. 5(a)–(c) shows the simulation result of proposed 3×3 , 5×5 , and 10×10 on-chip MIMO system, respectively. For these cases, the input optical power is attenuated from -17 to -23 dBm. The BER becomes smaller than 10^{-12} when the input optical power is larger than -18.72 , -18.37 , and -18.18 dBm in the case of 3×3 , 5×5 , and 10×10 , respectively. However, the input optical powers at the BER of 10^{-12} (error-free data transmission) are a little different between each channel in each MIMO systems. To observe this phenomenon, Fig. 5(d) shows the Box chart of input optical power at the BER of 10^{-12} for each MIMO system. The variation range slightly increases when the number of waveguides increases. The optical power variations at BER of 10^{-12} are 1.27, 4.2, and 5.02 μW for the case of 3×3 , 5×5 , and 10×10 , respectively. It's due to the slight disturbance caused by the randomly noise in each transmitter channel, and it leads to the BER variation among the receiver channels.

Since the coherent detection is utilized in the receiver, the local oscillator has to lock the phase of incoming signal in the coherent detection. Any phase error between the transmit lasers and the local oscillator, which are generally caused by phase noises when different lasers are used for transmitters and local oscillators, will decrease the performance of coherent detection and therefore affecting the capability of MIMO technique. Unfortunately, such phase noises are not predictable in the on-chip

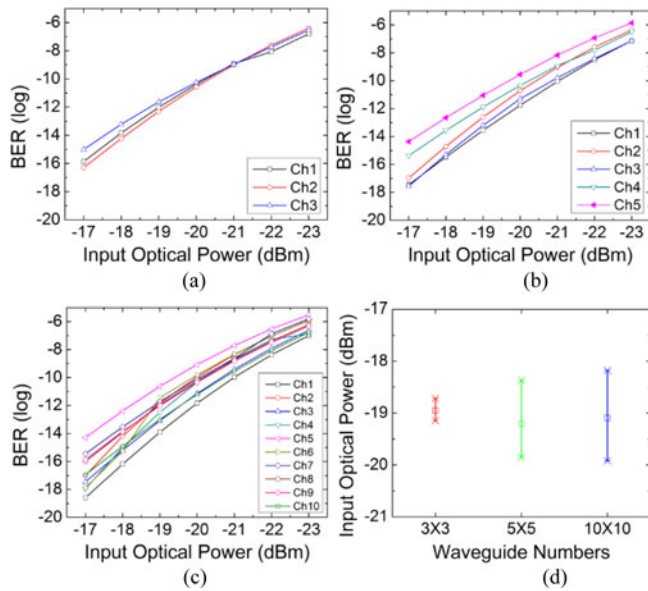


Fig. 5. The simulated BER as a function of the input optical power for the (a) 3×3 , (b) 5×5 , and (c) 10×10 on-chip MIMO systems. The BER could be smaller than 10^{-12} when the received optical power is larger than -18.1 dBm. (d) The Box chart of input optical power at the BER of 10^{-12} for each MIMO system.

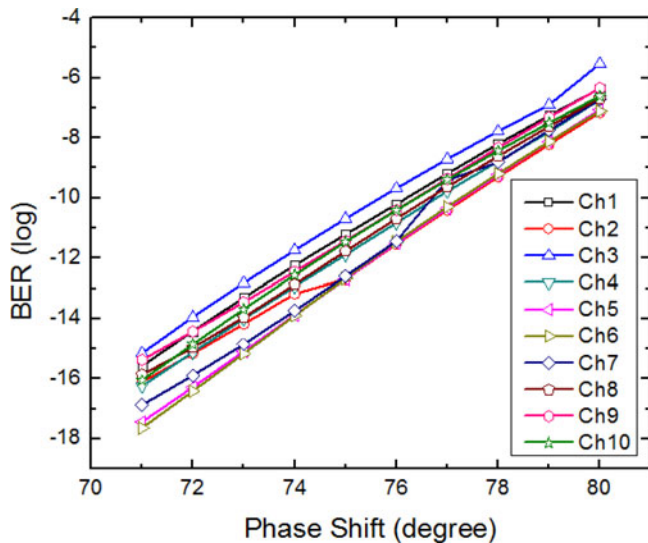


Fig. 6. The simulated BER as a function of the phase shift between input laser and local oscillator. The maximum phase shift is 73.5° when BER is greater than 10^{-12} .

MIMO systems so that it cannot be included in the transfer matrix. In order to verify the performance of coherent detection for the 10×10 on-chip MIMO system, we simplify the problem and consider the high density waveguides as ideal waveguides. We synchronously adjust the phase of all local oscillators to imitate the phase shift between input laser and local oscillator. Fig. 6 shows the BER as the function of phase shift between input laser and local oscillator. The simulations indicate that the BER is still better than 10^{-12} when there is a phase shift of 73.5° . There are some BER variations among each channel,

because each input channel has an independent electrical signal source and a randomly electrical noise source in the simulation. Although each optical signal emitted from the transmitter has the same quality factor, but these channels have different noise distribution due to the independent noise source. These random noise distribution would induce the BER variation when the coherent detection is used to decode the transmitted signal.

IV. CONCLUSION

In conclusion, we for the first time propose to apply the MIMO in wireless communication to high density on-chip optical interconnect. The simulation shows that it is possible to recover 10 Gb/s/channel data rate from 10 heavily coupled waveguides with 250 nm spacing. The BER is better than 10^{-12} , and the minimum input optical power for a BER of 10^{-12} is greater than -18.1 dBm assuming realistic optical link parameters. The BER is better than 10^{-12} when there is a phase shift of 73.5° . With MIMO, the waveguide pitch could be significantly reduced to subwavelength range and make it possible to increase the bandwidth density. Although, the proposed on-chip MIMO needs signal processing to recover entangled signals, the tradeoff between signal processing overhead and benefit of bandwidth density improvement should be manageable and certainly worth the effort. In the future, the electrical demultiplexer may be introduced in the receiver to release the bandwidth limitation of signal processing, so that the data rate of each waveguide channel can be improved and further enhance the bandwidth density.

ACKNOWLEDGMENT

The authors would like to appreciate the assistance of Dr. R. C. Daniels, Kumar Signals, LLC, in developing the signal processing.

REFERENCES

- [1] D. A. B. Miller, "Device requirements for optical interconnects to silicon chips," *Proc. IEEE*, vol. 97, no. 7, pp. 1166–1185, Jul. 2009.
- [2] R. G. Beausoleil, P. J. Kuekes, G. S. Snider, S. Y. Wang, and R. S. Williams, "Nanoelectronic and nanophotonic interconnect," *Proc. IEEE*, vol. 96, no. 2, pp. 230–247, Feb. 2008.
- [3] L. W. Luo, N. Ophir, C. P. Chen, L. H. Gabrielli, C. B. Poitras, K. Bergmen, and M. Lipson, "WDM-compatible mode-division multiplexing on a silicon chip," *Nature Commun.*, vol. 5, pp. 3069–1–3069–7, Jan. 2014.
- [4] J. Wang, S. He, and D. Dai, "On-chip silicon 8-channel hybrid (de)multiplexer enabling simultaneous mode- and polarization-division-multiplexing," *Laser Photon. Rev.*, vol. 8, no. 2, pp. L18–L22, Mar. 2014.
- [5] M. Haurylau, G. Chen, H. Chen, J. Zhang, N. A. Nelson, D. H. Albonese, E. G. Friedman, and P. M. Fauchet, "On-chip optical interconnect roadmap: Challenges and critical directions," *IEEE J. Sel. Topics Quantum Electron.*, vol. 12, no. 6, pp. 1699–1705, Dec. 2006.
- [6] G. Li, J. Yao, Y. Luo, H. Thacker, A. Mekis, X. Zheng, I. Shubin, J. H. Lee, K. Raj, J. E. Cunningham, and A. V. Krishnamoorthy, "Ultralow-loss, high-density SOI optical waveguide routing for macrochip interconnects," *Opt. Exp.*, vol. 20, no. 11, pp. 12035–12039, May 2012.
- [7] P. Dong, W. Qian, S. Liao, H. Liang, C. C. Kung, N. N. Feng, R. Shafiha, J. Fong, D. Feng, A. V. Krishnamoorthy, and M. Asghari, "Low loss shallow-ridge silicon waveguides," *Opt. Exp.*, vol. 18, no. 14, pp. 14474–14479, Jun. 2010.
- [8] Y. Liu, J. M. Shainline, X. Zeng, and M. A. Popović, "Ultra-low-loss CMOS-compatible waveguide crossing arrays based on multimode Bloch waves and imaginary coupling," *Opt. Lett.*, vol. 39, no. 2, pp. 335–338, Jan. 2014.

- [9] V. Donzella, S. T. Fard, and L. Chrostowski, "Study of waveguide crosstalk in silicon photonics integrated circuits," *Proc. SPIE*, vol. 8915, pp. 891502-1-891502-8, 2013.
- [10] R. G. H. van Uden, R. A. Correa, E. A. Lopez, F. M. Huijskens, C. Xia, G. Li, A. Schülzgen, H. de Waardt, A. M. J. Koonen, and C. M. Okonkwo, "Ultra-high-density spatial division multiplexing with a few-mode multicore fibre," *Nature Photon.*, vol. 8, pp. 865-870, Nov. 2014.
- [11] K. Appaiah, S. Vishwanath, and S. R. Bank, "Device design and signal processing for multiple-input multiple-output multimode fiber links," *Proc. SPIE*, vol. 8267, pp. 826715-1-826715-7, 2012.
- [12] R. C. J. Hsu, A. Tarighat, A. Shah, A. H. Sayed, and B. Jalali, "Capacity enhancement in coherent optical MIMO (COMIMO) multimode fiber links," *IEEE Commun. Lett.*, vol. 10, no. 3, pp. 195-197, Mar. 2006.
- [13] A. Tarighat, R. C. J. Hsu, A. Shah, A. H. Sayed, and B. Jalali, "Fundamentals and challenges of optical multiple-input multiple-output multimode fiber links," *IEEE Commun. Mag.*, vol. 45, no. 5, pp. 57-63, May 2007.
- [14] A. R. Shah, R. C. J. Hsu, A. Tarighat, A. H. Sayed, and B. Jalali, "Coherent optical MIMO (COMIMO)," *J. Lightw. Technol.*, vol. 23, no. 8, pp. 2410-2419, Apr. 2005.
- [15] M. A. Jensen and J. W. Wallace, "A review of antennas and propagation for MIMO wireless communications," *IEEE Trans. Antennas Propag.*, vol. 52, no. 11, pp. 2810-2824, Nov. 2004.
- [16] D. Gesbert, M. Shafi, D. S. Shiu, P. J. Smith, and A. Naguib, "From theory to practice: An overview of MIMO space-time coded wireless systems," *IEEE J. Sel. Areas Commun.*, vol. 21, no. 3, pp. 281-302, Apr. 2003.
- [17] E. Ip, A. P. T. Lau, D. J. F. Barros, and J. M. Kahn, "Coherent detection in optical fiber systems," *Opt. Exp.*, vol. 16, no. 2, pp. 753-791, Jan. 2008.
- [18] I. H. Malitson, "Interspecimen comparison of the refractive index of fused silica," *J. Opt. Soc. Amer.*, vol. 55, no. 10, pp. 1205-1209, Oct. 1965.
- [19] P. J. Winzer and G. J. Foschini, "MIMO capacities and outage probabilities in spatially multiplexed optical transport systems," *Opt. Exp.*, vol. 19, no. 17, pp. 16680-16696, Aug. 2011.
- [20] Keysight Technologies. 81250 13.5 Gb/s ParBERT Modules (N4872A, N4873A). (2008). [Online]. Available: <http://www.keysight.com/en/pd-190396-pn-N4872A-ATO/135-gb-s-parbert-modules-n4872a-n4873a?cc=US&lc=eng>
- [21] Gooch & Housego Enabling photonic Technologies. EM750 Narrow-Linewidth DFB Laser Module. (2014). [Online]. Available: <http://goochandhousego.com/product/narrow-linewidth-dfb-laser-modules/>
- [22] W. Bogaerts, S. K. Selvaraja, P. Dumon, J. Brouckaert, K. D. Vos, D. V. Thourhout, and R. Baets, "Silicon-on-insulator spectral filters fabricated with CMOS technology," *J. Sel. Topics Quant. Electron.*, vol. 16, no. 1, pp. 33-44, Feb. 2010.
- [23] M. Seimetz and C. M. Weinert, "Options, feasibility, and availability of 2×4 90° hybrids for coherent optical systems," *J. Lightw. Technol.*, vol. 24, no. 3, pp. 1317-1322, Mar. 2006.
- [24] L. Vivien, J. Osmond, J. M. Fédéli, M. M. Delphine, P. Crozat, J. F. Damlencourt, E. Cassan, Y. Lecunff, and S. Laval, "42 GHz p.i.n Germanium photodetector integrated in a silicon-on-insulator waveguide," *Opt. Exp.*, vol. 17, no. 8, pp. 6252-6257, Apr. 2009.

Po-Kuan Shen received the B.S. degree in physics from the National Chiayi University, Chiayi City, Taiwan, and the M.S. degree in optical sciences from the National Central University, Taoyuan City, Taiwan, in 2008 and 2010, respectively. He is currently working toward the Ph.D. degree in the Department of Optics and Photonics, National Central University, Taiwan. His research interests include photonic integrated circuits, and optical interconnects.

Amir Hosseini (S'05-M'13) received the B.Sc. degree in electrical engineering from the Sharif University of Technology, Tehran, Iran, in 2005, the M.Sc. degree in electrical and computer engineering in 2007 from Rice University, Houston, TX, USA, and the Ph.D. degree in electrical and computer engineering from the University of Texas at Austin, Austin, TX, USA, in 2011.

He has been engaged in research on modeling, design, fabrication, and characterization of optical phased array technology, true-time delay lines, and high-performance optical modulators. He is a Prince of Wales' scholar in 2011 and received the Ben Streetman Award in 2012, and has authored or coauthored more than 100 peer reviewed technical papers. He is a Member of the Optical Society of America and International Society for Optical Engineers. He has been serving as the Principal Investigator for an Air Force Research Laboratory sponsored project on polymer optical modulators since 2012.

Xiaochuan Xu (M'15) received the B.Sc. and M.S. degrees in electrical engineering from the Harbin Institute of Technology, Harbin, China, in 2006 and 2009, respectively, and the Ph.D. degree in electrical and computer engineering from the University of Texas, Austin, TX, USA, in 2013.

His research interests include flexible photonics, nonlinear optics, fiber optics, and silicon photonics.

Yongqiang Hei received the B.Sc. and Ph.D. degrees in telecommunication engineering from the Xidian University, Xi'an, China, in 2006 and 2010, respectively. From 2010, he worked in Xidian University as a teacher. His research interests include MIMO, cognitive radio, resource allocation in wireless communication.

Zeyu Pan (S'12) received the B.S. degree in optical information science and technology from the Nanjing University of Science and Technology, Nanjing, China, in 2010, and the M.S. degree in electrical and computer engineering from the University of Alabama in Huntsville, Huntsville, AL, USA, in 2013. He is currently working toward the Ph.D. degree in the University of Texas at Austin, Austin, TX, USA. He has authored and coauthored about 25 journal and conference publications. His interests include the polymer waveguide, printed flexible electronics and photonics, patch array antennas, thermo- and electro-optic polymers, phase delay, nanofabrication, RF measurements, inkjet printing, imprinting, and numerical algorithms.

Ray T. Chen (M'91-SM'98-F'04) received the B.S. degree in physics from the National Tsing Hua University, Hsinchu City, Taiwan, in 1980, the M.S. degree in physics in 1983, and the Ph.D. degree in electrical engineering in 1988, both from the University of California, Sacramento, CA, USA. He holds the Keys and Joan Curry/Cullen Trust Endowed Chair at The University of Texas Austin. He is the Director of the Nanophotonics and Optical Interconnects Research Lab, at the Microelectronics Research Center.

He is also the Director of the newly formed AFOSR MURI-Center for Silicon Nanomembrane involving faculty from Stanford, UIUC, Rutgers, and UT Austin. He joined UT Austin in 1992 to start the optical interconnect research program. From 1988 to 1992, he was a Research Scientist, Manager, and the Director of the Department of Electro-Optic Engineering, Physical Optics Corporation in Torrance, CA, USA.

He was the CTO, Founder, and Chairman of the Board of Radiant Research, Inc. from 2000 to 2001, where he raised 18 million dollars A-Round funding to commercialize polymer-based photonic devices involving over 20 patents, which were acquired by Finisar in 2002, a publicly traded company in the Silicon Valley (NASDAQ:FNSR). He also was the Founder and Chairman of the Board of Omega Optics Inc. since its initiation in 2001. Omega Optics has received over five million dollars in research funding.

His research work has been awarded more than 120 research grants and contracts from such sponsors as Army, Navy, Air Force, DARPA, MDA, NSA, NSF, DOE, EPA, NIH, NASA, the State of Texas, and private industry. The research topics are focused on three main subjects: 1) Nano-photonics passive and active devices for sensing and interconnect applications, 2) Thin film guided-wave optical interconnection and packaging for 2-D and 3-D laser beam routing and steering, and 3) True time delay wide band phased array antenna (PAA). Experiences garnered through these programs in polymeric and semi-conducting material processing and device integration are pivotal elements for his research work.

His group at UT Austin has reported its research findings in more than 780 published papers, including over 85 invited papers. He holds 25 issued patents. He has chaired or been a program-committee member for more than 110 domestic and international conferences organized by IEEE, The International Society of Optical Engineering, OSA, and PSC. He has served as an Editor, Co-editor or Coauthor for more than 20 books. He has also served as a Consultant for various federal agencies and private companies and delivered numerous invited talks to professional societies. He is a Fellow of the OSA and SPIE. He received the 1987 UC Regent's Dissertation Fellowship and the 1999 UT Engineering Foundation Faculty Award, for his contributions in research, teaching and services. He also received the 2008 IEEE Teaching Award, and the 2010 IEEE HKN Loudest Professor Award, 2013 NASA Certified Technical Achievement Award for contribution on moon surveillance conformable PAA. During his undergraduate years at the National Tsing Hua University, he led the 1979 university debate team to the Championship of the Taiwan College-Cup Debate Contest.

He has supervised and graduated 46 Ph.D. students from his research group at UT Austin.